DALTON
FULL PAPER

The first systematic stability study of mononuclear and dinuclear iron(II) and iron(III) complexes incorporating a dinucleating macrocyclic ligand in aqueous solution †

Zheng Wang, Arthur E. Martell,* Ramunas J. Motekaitis and Joseph Reibenspies

Department of Chemistry, Texas A&M University, College Station, Texas 77842-3012

Received 16th October 1998, Accepted 3rd June 1999

The dinucleating 24-membered hexaazadiphenol macrocyclic ligand 15,31-dimethyl-3,11,19,27,33,35-hexaaza-pentacyclo[27.3.1.1.^{5,9}1.^{13,17}1.^{21,25}]-hexatriaconta-5,7,9(33),13,15,17(34),21,23,25(35),29,31,1(36)-dodecaene-34,36-diol ([24]RBPyBC), prepared by the $NaBH_4$ reduction of the Schiff base obtained from the [2 + 2] condensation between 2,6-diformylpyridine and 2,6-bis(aminomethyl)-*p*-cresol, forms a variety of anionic and cationic species in aqueous solution. The structure of ([24]RBPyBC)·4HCl·6CH_3OH was determined by X-ray crystallographic methods. The ligand maintains dinuclear integrity for both iron(II,II) and iron(III, III) states, while facilitating the formation of bridging μ-phenolate diiron cores. Potentiometric equilibrium studies indicate that a variety of protonated, mononuclear and dinuclear iron(II) and iron(III) complexes form through p[H] 2 to 11 in aqueous solution. The protonation constants of the ligand and all associated stability constants of the 1 : 1, 1 : 2 [ligand:iron(II) or iron(III)], and 1 : 1 : 1 [ligand : iron(II) : iron(III)] complexes were determined in KCl supporting electrolyte (0.100 M) at 25.0 °C. The mechanisms of the formation of dinuclear iron(II), iron(III) and the mixed-valence iron(II,III) complexes are described.

Introduction

Dinuclear iron centers have been found in hemerythrin, methane monooxygenase, and the B_2 subunits of ribonucleotide reductase.[1] These proteins have elicited interest because of their widespread occurrence and the diverse nature of their functions, including reversible O_2 binding, alkane hydroxylation, and DNA biosynthesis.[2]

During the last decade, synthetic structural models for these proteins using several types of ligand have appeared in the literature[3] in recognition of the role played by dinuclear iron centers in metalloproteins. The synthetic dinuclear iron complexes of a large body of facially capped tridentate or tetradentate ligands,[4] alkoxo-bridging polypodal ligands[5] and a few dinucleating macrocyclic ligands[6] have contributed much to our understanding of the behavior of coupled diiron systems. In recent years, two 20-membered tetraazadiphenol macrocyclic ligands (see Fig. 1, H_2L_I and H_2L_{II}) were used to study diiron as well as other dinuclear transition metal (M^{2+}) complexes, in which $L_IM^{2+}M^{2+}$, $L_{II}M^{2+}Fe^{3+}$, and $L_{II}Fe^{3+}$-$(OH)_2Fe^{3+}L_{II}$ species were successfully prepared.[7] However, the dinuclear species containing two Fe(III) ions within a single macrocycle could not be obtained. The tripositively-charged centers Fe^{3+}, Fe^{3+} cannot be held together in the 20-membered macrocycle because of the strong coulombic repulsion between the Fe(III) centers that would be imposed in such a structure.

In order to study the various oxidation states of the dinuclear iron site in a preorganized arrangement, specially designed dinucleating macrocyclic ligands need to be developed. Recently, we have widened the scope of the available dinucleating ligands by designing larger macrocycles containing more donor groups which are known to have special affinity for ferrous and ferric centers.[8] Such ligands are the 24-membered hexaazadiphenol and 30-membered octaazadiphenol macrocycles (See Fig. 1, H_2L_{III}, H_2L_{IV}, H_2L_V and H_2L_{VI}).[9] As part of the continuing studies of the new series of dinucleating macrocyclic ligands[10] and their homonuclear and heteronuclear transition metal complexes, we report here the X-ray crystal structure of one such macrocyclic ligand, [24]RBPyBC (hereafter H_2L_{IV}).

In contrast to tetraimine Schiff base ligands (H_2L_I, H_2L_{III}, H_2L_V), one advantage of the corresponding tetraamine ligands (H_2L_{II}, H_2L_{VI}) is that they can be studied in aqueous solution, the natural medium of enzymes. Moreover, the dinuclear metal models incorporating the more flexible polyamine ligands may allow metal–metal spatial distances and coordination geometry to vary from one intermediate to the next. Regarding the different coordination chemistries of these ligands, the pairs of enlarged 24-membered macrocycles H_2L_{III} and H_2L_{IV} along with the 30-membered analogs H_2L_V and H_2L_{VI}, provide two sets of macrocyclic ligands that closely parallel the 20-membered systems H_2L_I and H_2L_{II}.

The stepwise stability constants of mononuclear and dinuclear complexes formed by iron(II) and iron(III) with [24]RBPyBC from p[H] 2 to 11 (where p[H] represents $-\log[H^+]$) were determined and discussed in this paper. This constitutes a major addition to the work reported on dinuclear iron(II) and iron(III) complexes in aqueous solution.[6]

Results and discussion

H_2L_{IV}·4HCl

In our previously published procedure,[9] the ligand was recrystallized from methanolic solution containing 32% HCl as an approximate hexahydrochloride salt in which the HCl content was not quite reproducible because the pyridine nitrogens of the ligand are difficult to protonate completely. In order to obtain the ligand sample with a reproducible chemical composition for titration studies, a methanolic solution containing 5% HCl was employed to prepare the ligand as a tetrahydrochloride salt. Drying *in vacuo* followed by re-exposure to the atmosphere gave a solid of composition

† *Supplementary data available*: UV-visible spectra of [24]RBPyBC. For direct electronic access see http://www.rsc.org/suppdata/dt/1999/2441/, otherwise available from BLDSC (No. SUP 57573, 1 pp.) or the RSC library. See Instructions for Authors, 1999, Issue 1 (http://www.rsc.org/dalton).

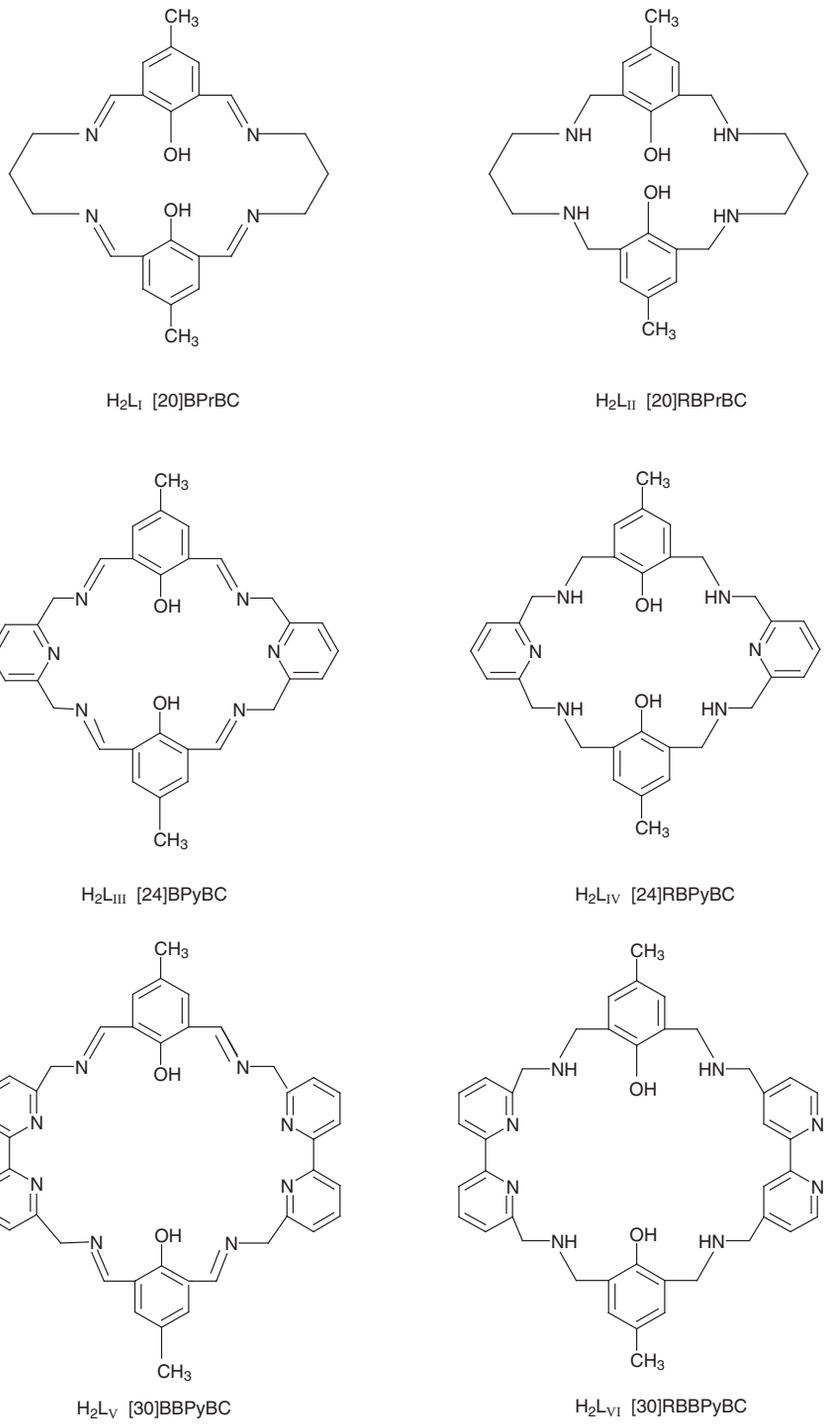

Fig. 1 Polyazadiphenol dinucleating macrocyclic ligands.

H_2L_{IV}·4HCl·1/3CH_3OH·5/3H_2O by elemental analysis (F.W. = 725), which agrees with the results found by potentiometric titration (F.W. = 722).

A single crystal suitable for X-ray crystallography with the composition H_2L_{IV}·4HCl·6CH_3OH, **1**, was obtained by recrystallization from methanol. Fig. 2 shows the structure and the atom-numbering scheme of the macrocyclic tetracation $H_6L_{IV}^{4+}$, together with the associated four chloride ions and the six methanol molecules which are involved in a complex hydrogen-bonded network. Selected interatomic distances and angles are given in Table 1.

The X-ray crystallographic analysis of **1** (see Fig. 2) shows that all four amino nitrogens of the macrocycle are protonated but not the two pyridyl nitrogens, which were fully protonated in the previously determined structure of the heptahydrobromide salt of this ligand.[9] The $H_6L_{IV}^{4+}$ cation adopts a parallelogram arrangement with two phenolic oxygen atoms and two pyridyl nitrogen atoms oriented toward the center of the macrocycle and the aromatic groups at the farther corners. The four amino nitrogens lie on a perfect plane of the inherent crystal symmetry. The two pyridines are inclined equally to this N_4 plane, with a dihedral angle of 38.4°. The two aromatic phenolic rings are also inclined to the N_4 plane, with a dihedral angle of 29.2°.

The macrocycle is shaped by internal hydrogen bonding so that the ligand molecule adopts a central symmetry in the space group $P\bar{1}$. Though a hydrogen atom associated with O(1) was not observed in the crystal structure analysis, the short distance between O(1) and Cl(2) was strongly suggestive of hydrogen bonding [O(1)···Cl(2), 3.02(1) Å].[11] As is indicated in Table 1, N(1) and N(3) are hydrogen bonded to Cl(1) [N(1)···Cl(1), 3.20(1); N(3)···Cl(1), 3.07(1) Å], and also to N(2) [N(1)···

Table 1 Selected interatomic distances (Å) and angles (°) for H_2L_{IV}·4HCl·6CH_3OH [a]

O1 · · · Cl2	3.02(1)	N1 · · · Cl1	3.20(1)
N3 · · · Cl1	3.07(1)	N1 · · · N2	2.65(1)
N3 · · · N2	2.75(1)	O3 · · · Cl2	3.14(1)
O4 · · · Cl2	3.07(1)	O1 · · · N2	3.21(1)
O1 · · · Cl1	3.36(1)	O2 · · · O4	2.74(1)
O(1)–C(15)	1.368(7)	C(4)–C(5)	1.359(9)
O(2)–C(17)	1.379(8)	C(5)–C(6)	1.382(9)
O(3)–C(18)	1.383(8)	C(6)–C(7)	1.368(8)
O(4)–C(19)	1.374(8)	C(7)–C(8)	1.501(8)
N(1)–C(2)	1.476(7)	C(9)–C(10)	1.506(7)
N(1)–C(1)	1.518(7)	C(10)–C(15)	1.381(8)
N(2)–C(3)	1.317(7)	C(10)–C(11)	1.391(8)
N(2)–C(7)	1.350(7)	C(11)–C(12)	1.400(8)
N(3)–C(8)	1.502(7)	C(12)–C(13)	1.381(9)
N(3)–C(9)	1.504(7)	C(12)–C(16)	1.492(8)
C(1)–C(14)[b]	1.477(8)	C(13)–C(14)	1.392(8)
C(2)–C(3)	1.500(8)	C(14)–C(15)	1.415(7)
C(3)–C(4)	1.396(8)	C(14)–C(1)[b]	1.477(8)
C(2)–N(1)–C(1)	115.3(4)	N(3)–C(9)–C(10)	109.6(4)
C(3)–N(2)–C(7)	118.3(5)	C(15)–C(10)–C(11)	118.3(5)
C(8)–N(3)–C(9)	115.2(4)	C(15)–C(10)–C(9)	120.4(5)
C(14)[b]–C(1)–N(1)	109.6(5)	C(11)–C(10)–C(9)	121.0(6)
N(1)–C(2)–C(3)	110.8(5)	C(10)–C(11)–C(12)	122.9(6)
N(2)–C(3)–C(4)	122.1(6)	C(13)–C(12)–C(11)	116.5(6)
N(2)–C(3)–C(2)	117.0(5)	C(13)–C(12)–C(16)	122.1(5)
C(4)–C(3)–C(2)	120.7(6)	C(11)–C(12)–C(16)	121.3(6)
C(5)–C(4)–C(3)	118.9(6)	C(12)–C(13)–C(14)	123.4(5)
C(4)–C(5)–C(6)	119.5(5)	C(13)–C(14)–C(15)	117.5(6)
C(7)–C(6)–C(5)	118.4(6)	C(13)–C(14)–C(1)[b]	123.2(5)
N(2)–C(7)–C(6)	122.7(6)	C(15)–C(14)–C(1)[b]	119.2(5)
N(2)–C(7)–C(8)	114.7(5)	O(1)–C(15)–C(10)	122.8(5)
C(6)–C(7)–C(8)	122.5(6)	O(1)–C(15)–C(14)	116.0(5)
C(7)–C(8)–N(3)	110.2(5)	C(10)–C(15)–C(14)	121.2(6)

[a] Numbers in parentheses are standard deviations in the last significant digit. [b] Symmetry transformation used to generate equivalent atoms: $-x+1, -y+1, -z+1$.

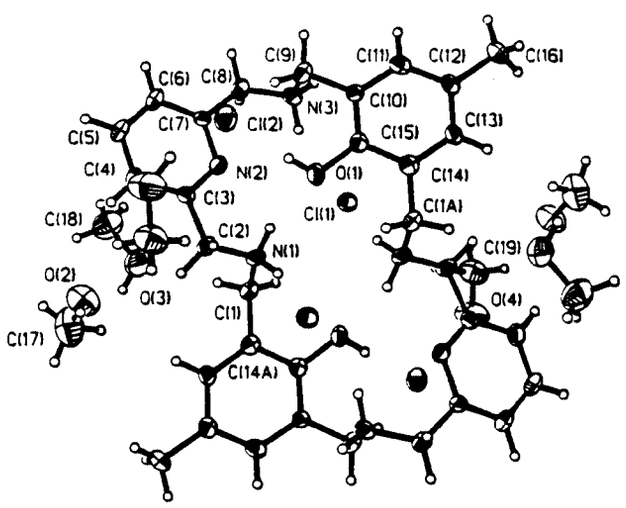

Fig. 2 Molecular structure of [24]RBPyBC·4HCl·6CH_3OH (**1**). Ellipsoids are drawn at the 50% probability level.

N(2), 2.65(1); N(3) · · · N(2), 2.75(1) Å]. Cl(2) is hydrogen bonded to the oxygen atoms of two methanol molecules [O(3) · · · Cl(2), 3.14(1); O(4) · · · Cl(2), 3.07(1) Å]. The O(2) of the methanol is solely involved in the hydrogen bonding to O(4) [O(2) · · · O(4), 2.74(1) Å] outside of the $H_6L_{IV}^{4+}$ macrocyclic cavity. The structure, therefore, could be described as $[(H_6L_{IV}^{4+})\cdot(Cl^-)_4]\cdot(CH_3OH)_6$. On the other hand, the structure of the heptahydrobromide salt of the ligand was determined crystallographically[9] as $[(H_8L_{IV}^{6+})(Br^-)_6\cdot H_3O^+]Br^-$. It is interesting to see that the ligand adopts various symmetries when the protonation and the solvation are changed.

Table 2 Successive protonation constants of [24]RBPyBC, HBED,[a] and C-BISBAMP[b]

	[c] $\log K_i^H$			
i	[24]RBPyBC[d]	HBED[f]	i	C-BISBAMP[g]
1	12.1[e]	12.6		
2	11.3[e]	11.0		
3	9.18	8.44	1	9.11
4	8.92	4.72	2	8.32
5	6.65	2.53	3	7.12
6	4.52	1.7	4	3.72

[a] HBED = *N*,*N*′-di(2-hydroxybenzyl)ethylenediamine-*N*,*N*′-diacetic acid. [b] C-BISBAMP = 3,8,16,21,27,28-hexaazatricyclo[21.3.1.1^{10,14}]-octacosa-1(26),10(28),11,13,23(27),24-hexaene. [c] $K_i^H = [H_iL^{i-2}]/[H]-[H_{i-1}L^{i-3}]$. [d] This work ($\mu = 0.100$ M (KCl), 25.0 °C), Standard deviation = ±0.04. [e] This work, UV-visible measurement, estimated error = ±0.1. [f] Reference 12(*a*,*b*) ($\mu = 0.100$ M (KNO_3), $T = 25$ °C). [g] Reference 12(*c*) ($\mu = 0.0100$ M ($NaClO_4$), $T = 25$ °C).

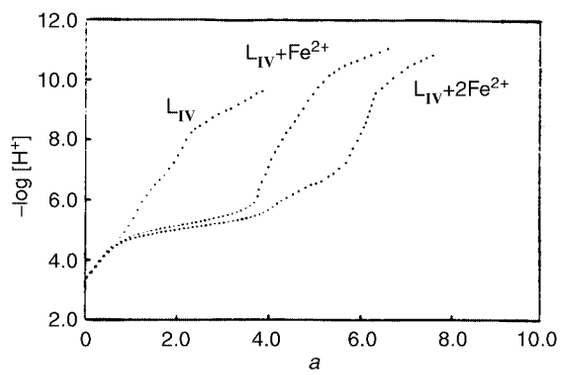

Fig. 3 Potentiometric equilibrium curves for L_{IV}–Fe(II) systems in argon at 25.00 ± 0.05 °C and $\mu = 0.100$ M (KCl): $T_L = 2.212 \times 10^{-3}$ M; $T_{Fe(II)} = 2.120 \times 10^{-3}$ M (1:1 Fe^{2+}–L_{IV}); $T_{Fe(II)} = 4.240 \times 10^{-3}$ M (2:1 Fe^{2+}–L_{IV}) [a = moles of standard KOH added per mole of ligand present].

Protonation constants of the ligand

The potentiometric curve for the ligand H_2L_{IV}·4HCl shown in Fig. 3 features a steeply sloping region from $a = 0$ to $a = 2$, where a is moles of base added per mole of ligand present in the experimental solution. This indicates two almost non-overlapping protonation equilibria. A smooth buffer region from $a = 2$ to almost $a = 4$ indicates two overlapping protonation equilibria. In this region, the neutral ligand remains in homogeneous supersaturated solution at 10^{-3} M levels. Above p[H] 10, precipitation of the neutral ligand occurred. Insolubility is indicated by a sudden discontinuity in p[H] readings, which can be detected before visual observation of the presence of the insoluble material. Such data were not used in the equilibrium calculations. Instead, the experiments were repeated several times in order to achieve supersaturation to the maximum extent possible. Above $a = 4$, a very low concentration (1.10×10^{-4} M) was studied spectrophotometrically and the data were analyzed by considering the variability of absorbance at 298 nm with p[H].

The combined results from both potentiometric and spectroscopic analyses for the protonation constants for this ligand are listed in Table 2. From a microscopic point of view, the values of the first and second protonation constants are essentially the phenolic protonations, while the third, fourth, fifth, and sixth ones should correspond to the protonations of the four aliphatic nitrogens. The pyridine nitrogens were found to be too weakly basic to become protonated under these experimental conditions. The stepwise protonation scheme is shown in Scheme 1 (only one microspecies is shown in all cases). At p[H] < 3, the ligand exists in the fully protonated form,

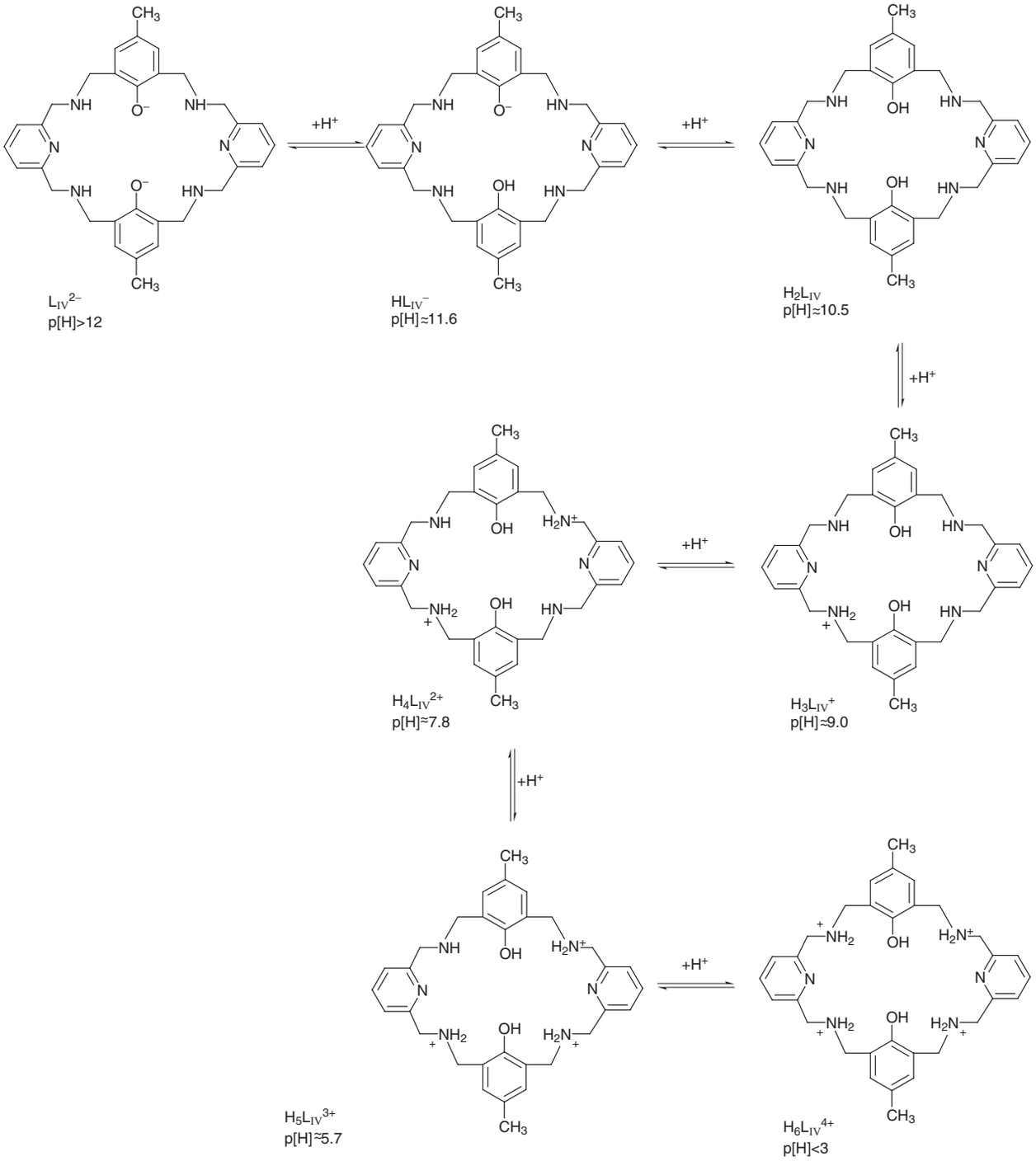

Scheme 1 Stepwise protonation diagram of L_{IV}^{2-}.

$H_6L_{IV}^{4+}$. As p[H] is increased, the macrocycle loses its protons from amino nitrogens to become $H_5L_{IV}^{3+}$, $H_4L_{IV}^{2+}$ and $H_3L_{IV}^{+}$ species respectively. The neutral ligand H_2L_{IV} reaches its maximum concentration (88%) at p[H] 10.5. Under more alkaline conditions, the two phenol groups finally deprotonate to form the free ligand dianion L_{IV}^{2-} (p[H] > 12).

To our knowledge, there are no examples of protonation constant studies of polyazadiphenol macrocyclic ligands in the literature.[8] Therefore acyclic ligands containing combinations of similar functional groups, HBED[12a,b] and C-BISBAMP,[12c] are included in Table 2 for comparison. HBED is a well-known bis(*o*-hydroxybenzyl) ligand which has a very high stability constant with Fe(III) and with other highly charged metal ions. The first two protonation constants of [24]RBPyBC and HBED are fairly close. Since there are two γ-amino groups adjacent to each phenolate in [24]RBPyBC exhibiting electron-withdrawing effects, instead of one γ-amino group as in HBED, it is reasonable that the first protonation constant of [24]RBPyBC (log $K_1^H = 12.1$) is 0.5 log units lower than that of the ligand HBED (log $K_1 = 12.6$). Since the two phenol groups of [24]RBPyBC are somewhat more separated than those of HBED, the difference in the first two protonation constants (log K_1^H − log $K_2^H = 0.8$) of [24]RBPyBC is smaller than that (log K_1^H − log $K_2^H = 1.6$) of HBED. In addition, the increase in absorbance around 300 nm that occurs in the conversion of one species to the next less protonated form is an indication of the participation of phenolate groups.[12a,b] HBED has been reported to have absorptions at $\lambda = 294$ nm with the following extinction coefficients for the three highest pH species: $\varepsilon_{L^{4-}} = 8300$, $\varepsilon_{HL^{3-}} = 4000$, $\varepsilon_{H_2L^{2-}} = 650$ M^{-1} cm^{-1}. In this work, [24]RBPyBC has absorptions at $\lambda = 298$ nm with the following extinction coefficients for the three highest pH species: $\varepsilon_{L_{IV}^{2-}} = 9000$, $\varepsilon_{HL_{IV}^{-}} =$

4900, $\varepsilon_{H_2L_{IV}} = 1200\ M^{-1}\ cm^{-1}$. The increases in absorptivities per protonation step for HBED and [24]RBPyBC are fairly parallel, indicating similar protonation patterns of phenolates in both ligands. As shown in Table 2, the log values of the protonation constants of [24]RBPyBC are also compared with those of C-BISBAMP which also has the 24-membered ring. The main difference between these ligands is the presence of the cresol groups in the bridges between the two BAMP moieties, so that the successive protonation constants of aliphatic nitrogens of [24]RBPyBC are fairly close to the corresponding ones of C-BISBAMP. The small variations can be ascribed to possible hydrogen bonding between phenolic oxygens and protonated nitrogens. The greater rigidity of [24]RBPyBC relative to that of C-BISBAMP is also expected to contribute to observed differences in the protonation constants.

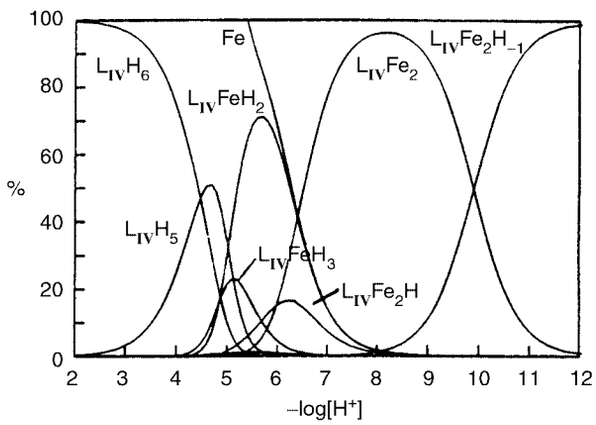

Fig. 4 Species distribution diagram for the L_{IV}–Fe(II) system as a function of p[H] ($Fe = Fe^{2+}$, $T_{Fe(II)} = 2T_{L_{IV}} = 4.00 \times 10^{-3}$ M). Only major species are shown: $L_{IV}H_4$ and $L_{IV}Fe_2H_2$ (1%) are omitted.

Table 3 Overall and stepwise stability constants for the L_{IV}–Fe(II) system [$\mu = 0.10$ M (KCl), 25.0 °C]

Stoichiometry L	Fe	H	Log β^a	Stepwise quotient K	Log K^a
1	1	0	15.32	$[L_{IV}Fe]/[L_{IV}][Fe]$	15.32
1	1	1	26.00	$[L_{IV}FeH]/[L_{IV}Fe][H]^b$	10.68
1	1	2	35.24	$[L_{IV}FeH_2]/[L_{IV}FeH][H]^b$	9.24
1	1	3	40.10	$[L_{IV}FeH_3]/[L_{IV}FeH_2][H]^b$	4.86
1	2	0	25.20	$[L_{IV}Fe_2]/[L_{IV}Fe][Fe]$	9.88
1	2	1	31.22	$[L_{IV}Fe_2H]/[L_{IV}Fe_2][H]^b$	6.02
1	2	−1	15.29	$[L_{IV}Fe_2]/[L_{IV}Fe_2(OH)][H]^{b,c}$	9.91

^{a} Estimated error = ±0.06. ^{b} H = H^+. ^{c} OH = OH^-.

Stability of mononuclear and dinuclear iron(II) complexes

The potentiometric data obtained for solutions containing H_2L_{IV}·4HCl and ferrous ion are illustrated in Fig. 3. The inflections at $a = 4.0$ and $a = 6.0$ indicate the formation of the mononuclear and dinuclear complexes, respectively. The p[H] titration curves were employed to calculate 1 : 1 and 1 : 2 ligand: metal binding constants, together with constants involving protonated, deprotonated, and hydroxo-bridged species shown in Table 3. Four mononuclear and three dinuclear complexes were identified with fairly high stability constants for the ferrous ion-ligand system. The species distribution diagram of the system $H_6L_{IV}^{4+}$–$2Fe^{II}$ is shown in Fig. 4. When p[H] < 5, the ligand exists as various protonated species in solution. Between p[H] 5 and 7, the mononuclear ferrous complex forms and reaches the maximum concentration (72%) at p[H] 5.7. The conversion of the 1 : 1 into 1 : 2 complexes occurs about p[H] > 7, when a second ferrous ion enters the same macrocycle to form dinuclear ferrous complexes (maximum concentration 94% at p[H] 8.1). Finally, the hydroxo-bridged species $[Fe^{II}_2(\mu\text{-}OH)L_{IV}]^+$ dominates when p[H] > 10.

Stability of mononuclear and dinuclear iron(III) complexes

Potentiometric equilibrium curves having 1 : 1 and 1 : 2 molar ratios of ligand to ferric ion are shown in Fig. 5. For the 1 : 1 system the strong inflection at $a = 4$ indicates the formation of the mononuclear ferric complex, $[Fe^{III}H_2L_{IV}]^{3+}$. For the 1 : 2 system a strong inflection occurs at $a = 7$ and 8, indicating that 2 mol of hydrogen ions were neutralized in addition to the 6 mol released from the ligand. This observation is evidence for the formation of the μ-hydroxo and μ-oxo bridges between two ferric ions in the dinuclear species even under fairly acidic conditions. This result is also consistent with the spectroscopic studies in aqueous solution. The overall and stepwise stability constants for the ligand–Fe(III) system are included in Table 4. Four mononuclear and five dinuclear complexes were identified with very high stability constants.

The species distribution diagram of the system $H_6L_{IV}^{4+}$–$2Fe^{III}$ is shown in Fig. 6. It is seen that the mononuclear $[Fe^{III}H_2L_{IV}]^{3+}$ complex predominates from p[H] 2 to 3. Then the other ferric ion coordinates to the macrocycle to form the dinuclear ferric complex $[Fe^{III}_2L_{IV}]^{4+}$ and reaches a maximum concentration (27%) at p[H] 3.1. Between p[H] 3.5 and 7, the stable μ-hydroxo bridged diferric complex $[Fe^{III}_2(\mu\text{-}OH)L_{IV}]^{3+}$ dominates. Above p[H] > 7, the μ-oxo bridged diferric complex $[Fe^{III}_2(\mu\text{-}O)L_{IV}]^{2+}$ and its further hydrolytic species become the main components in aqueous solution.

Stability of mixed-valence dinuclear iron(II, III) complexes

The pH profile for the 1 : 1 : 1 solutions of the ligand with Fe^{3+}

Table 4 Overall and stepwise stability constants for the L_{IV}–Fe(III) and the L_{IV}–Fe(III)–Fe(II) systems [$\mu = 0.10$ M (KCl), 25.0 °C], H = H^+, OH = OH^-

Stoichiometry L	Fe^{3+}	Fe^{2+}	H	Log β^a	Stepwise quotient K	Log K^a
1	1	0	0	32.02	$[L_{IV}Fe]/[L_{IV}][Fe]$	32.02
1	1	0	1	41.08	$[L_{IV}FeH]/[L_{IV}Fe][H]^b$	9.06
1	1	0	2	47.99	$[L_{IV}FeH_2]/[L_{IV}FeH][H]^b$	6.91
1	1	0	−1	22.06	$[L_{IV}Fe]/[L_{IV}Fe(OH)][H]^{b,c}$	9.96
1	2	0	0	44.9	$[L_{IV}Fe_2]/[L_{IV}Fe][Fe]$	12.89
1	2	0	−1	41.99	$[L_{IV}Fe_2]/[L_{IV}Fe_2(\mu\text{-}OH)][H]^{b,c}$	2.92
1	2	0	−2	34.65	$[L_{IV}Fe_2(\mu\text{-}OH)]/[L_{IV}Fe_2(\mu\text{-}O)][H]^b$	7.34
1	2	0	−3	25.64	$[L_{IV}Fe_2(\mu\text{-}O)]/[L_{IV}Fe_2(\mu\text{-}O)(OH)][H]^{b,c}$	9.01
1	2	0	−4	15.37	$[L_{IV}Fe_2(\mu\text{-}O)(OH)]/[L_{IV}Fe_2(\mu\text{-}O)(OH)_2][H]^{b,c}$	10.27
1	1	1	0	36.56	$[L_{IV}Fe^{3+}Fe^{2+}]/[L_{IV}Fe^{3+}][Fe^{2+}]$	4.54
1	1	1	−1	30.89	$[L_{IV}Fe^{3+}Fe^{2+}]/[L_{IV}Fe^{3+}Fe^{2+}(\mu\text{-}OH)][H]^{b,c}$	5.67
1	1	1	−2	21.60	$[L_{IV}Fe^{3+}Fe^{2+}(\mu\text{-}OH)]/[L_{IV}Fe^{3+}Fe^{2+}(OH)_2][H]^{b,c}$	9.29

^{a} Estimated error = ±0.06 or less. ^{b} H = H^+. ^{c} OH = OH^-.

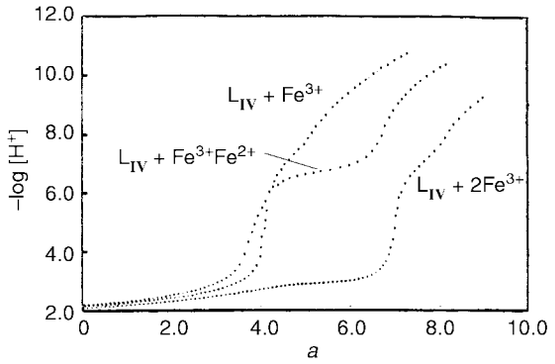

Fig. 5 Potentiometric equilibrium curves for L_{IV}–Fe(III, II) systems in argon at 25.00 ± 0.05 °C and μ = 0.100 M (KCl): $T_L = 2.212 \times 10^{-3}$ M, $T_{Fe(III)} = 2.201 \times 10^{-3}$ M (1:1 Fe^{3+}–L_{IV}); $T_{Fe(III)} = 4.402 \times 10^{-3}$ M (2:1 Fe^{3+}–L_{IV}); $T_{Fe(III)} = 1.966 \times 10^{-3}$ M, $T_{Fe(II)} = 2.120 \times 10^{-3}$ M (1:1:1 Fe^{3+}–Fe^{2+}–L_{IV}) [a = moles of standard KOH added per mole of ligand present].

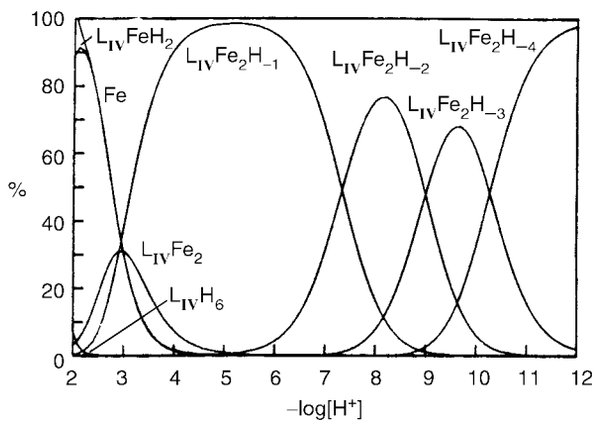

Fig. 6 Species distribution diagram for the L_{IV}–Fe(III) system as a function of p[H] (Fe = Fe^{3+}, $T_{Fe(III)} = 2T_{L_{IV}} = 4.00 \times 10^{-3}$ M). Only major species are shown; $L_{IV}FeH$, $L_{IV}Fe$ and $L_{IV}FeH_{-1}$ which are minor species (1%) are omitted.

and Fe^{2+} (Fig. 5) shows an inflection at $a = 4$ indicative of the initial formation of the mononuclear $[Fe^{III}H_2L_{IV}]^{3+}$ complex and an inflection at $a = 6$ indicative of the formation of the mixed-valence $[Fe^{III}Fe^{II}L_{IV}]^{3+}$ complex. In addition, the μ-hydroxo bridged mixed-valence species, $[Fe^{III}Fe^{II}(\mu\text{-}OH)L_{IV}]^{2+}$, and the corresponding dihydroxo species $[Fe^{III}Fe^{II}(OH)_2L_{IV}]$, are also identified and the stability constants for these species are included in Table 4.

From a coordination point of view, the ligand (Fig. 2) contains six nitrogens able to act as donor atoms in complexes, but they are arranged as two subunits separated by two phenolic bridging donor groups. It is expected that a mononuclear complex $[Fe^{III}H_2L_{IV}]^{3+}$ will be formed by the coordination of the ferric ion to one of the subunits (Scheme 2). Because of the low flexibility of the aromatic rings in the macrocycle, the amino nitrogens in the other subunit remain protonated in acidic solution. When the p[H] is raised, the amino groups deprotonate and finally the ferrous ion coordinates the donor groups on the other side of the macrocycle to form the mixed-valence complex. Finally the μ-hydroxo bridged species and further hydrolytic mixed-valence species are subsequently formed in alkaline solution.

The stability of the mixed-valence complex formed from dinuclear iron(III) and dinuclear iron(II) complexes is indicated by its comproportionation constant for the following equilibrium.[13]

$$[Fe^{III}{}_2L_{IV}]^{4+} + [Fe^{II}{}_2L_{IV}]^{2+} \rightleftharpoons 2[Fe^{III}Fe^{II}L_{IV}]^{3+} \quad (1)$$

$$K_{com} = ([Fe^{III}Fe^{II}L_{IV}]^{3+})^2/[Fe^{III}{}_2L_{IV}]^{4+}[Fe^{II}{}_2L_{IV}]^{2+} \quad (2)$$

From the stability constants of dinuclear ferrous, ferric and mixed-valence complexes listed in Table 3 and Table 4, the comproportionation constant ($K_{com} = 1.8 \times 10^4$) is calculated for equilibrium (1) in aqueous solution. The magnitude of K_{com} indicates that a mixture of single valence complexes is less stable than the mixed-valence diiron complexes of the polypodal ligands containing phenolate bridging groups. For example, $K_{com} = 4 \times 10^6$ for the $[Fe^{II}Fe^{III}(BBPPNOL)(\mu\text{-}OAc)_2]^+$ complex [BBPPNOL = *N*,*N*′-bis(2-hydroxybenzyl)-*N*,*N*′-bis(2-pyridylmethyl-2-hydroxy)-1,3-propanediamine] and $K_{com} = 8 \times 10^9$ for the $[Fe^{II}Fe^{III}(BBPMP)(\mu\text{-}OAc)_2]^+$ complex (BBPMP = 2,6-bis-{[(2-hydroxybenzyl)(2-pyridylmethyl)amino]methyl}-4-methylphenol).[13] Macrocyclic effects and coulombic interactions might be the most probable factors in the stabilization of these mixed-valence complexes.

Summary and perspectives

We have synthesized and characterized a 24-membered hexaazadiphenol macrocyclic ligand [24]RBPyBC. A single-crystal structure was obtained for the ligand with the formula $[(H_6L_{IV}{}^{4+})\cdot(Cl^-)_4]\cdot 6CH_3OH$. The protonation constants of the ligand and stability constants of mononuclear Fe^{II} and Fe^{III} complexes, and stability constants of dinuclear $Fe^{II}{}_2$, $Fe^{III}{}_2$, and $Fe^{II}Fe^{III}$ complexes have been determined by potentiometric and spectroscopic titration in aqueous solution. This is the first systematic study of both diferrous and diferric model compounds having high stabilities in water. The results have provided useful information about the formation of the diiron complexes in aqueous solution at various pH values and their quantitative stabilities. The high stabilities of these complexes also raise interest in future work on dinuclear complexes of other transition metals with this remarkable ligand, including heterobimetallic species such as $Fe^{III}Co^{II}$, $Fe^{III}Ni^{II}$, $Fe^{III}Cu^{II}$, $Fe^{III}Zn^{II}$, and $Fe^{III}Mn^{II}$, by the method used for the preparation of the mixed-valence $Fe^{III}Fe^{II}$ species. The dinuclear iron(II) complex of the ligand has been found to have catalytic properties for the hydroxylation of alkanes with molecular oxygen as an oxidant and H_2S as a two-electron reductant. The diiron complex thus serves as a functional model for MMO.[14] Some of this research is in progress in this laboratory and will be the subject of future reports.

Experimental

Materials

The synthesis and purification of the dinucleating macrocyclic ligand [24]RBPyBC was based in part on a previously published method.[9] $FeCl_3\cdot 6H_2O$ was purchased from Aldrich Chemical Co. and was used without further purification. Light green crystalline $FeCl_2$ was prepared under nitrogen by the direct reaction of concentrated hydrochloric acid with 99.9% iron chips. The stock solutions of iron(II) and iron(III) were prepared from crystalline $FeCl_2$ and analytical grade $FeCl_3$ in the presence of 0.0100 M hydrochloric acid. The concentrations of all above stock solutions were quantified by cation exchange techniques (Dowex 50W X8 cation exchange resin 20–50 mesh, hydrogen form). Solvents were appropriately purified, dried, and degassed. Where anaerobic conditions were required, an argon glove-box and standard Schlenk techniques were employed.

Physical measurements

Elemental analyses were measured by Galbraith Laboratories, Inc., Knoxville, TN. NMR spectra were measured with a Varian XL200 FT spectrometer. Chemical shifts are reported as δ(in ppm) relative to external tetramethylsilane or internal solvent. Mass spectra (FAB^+) were obtained with a VG analytical 70s high resolution double focusing magnetic sector

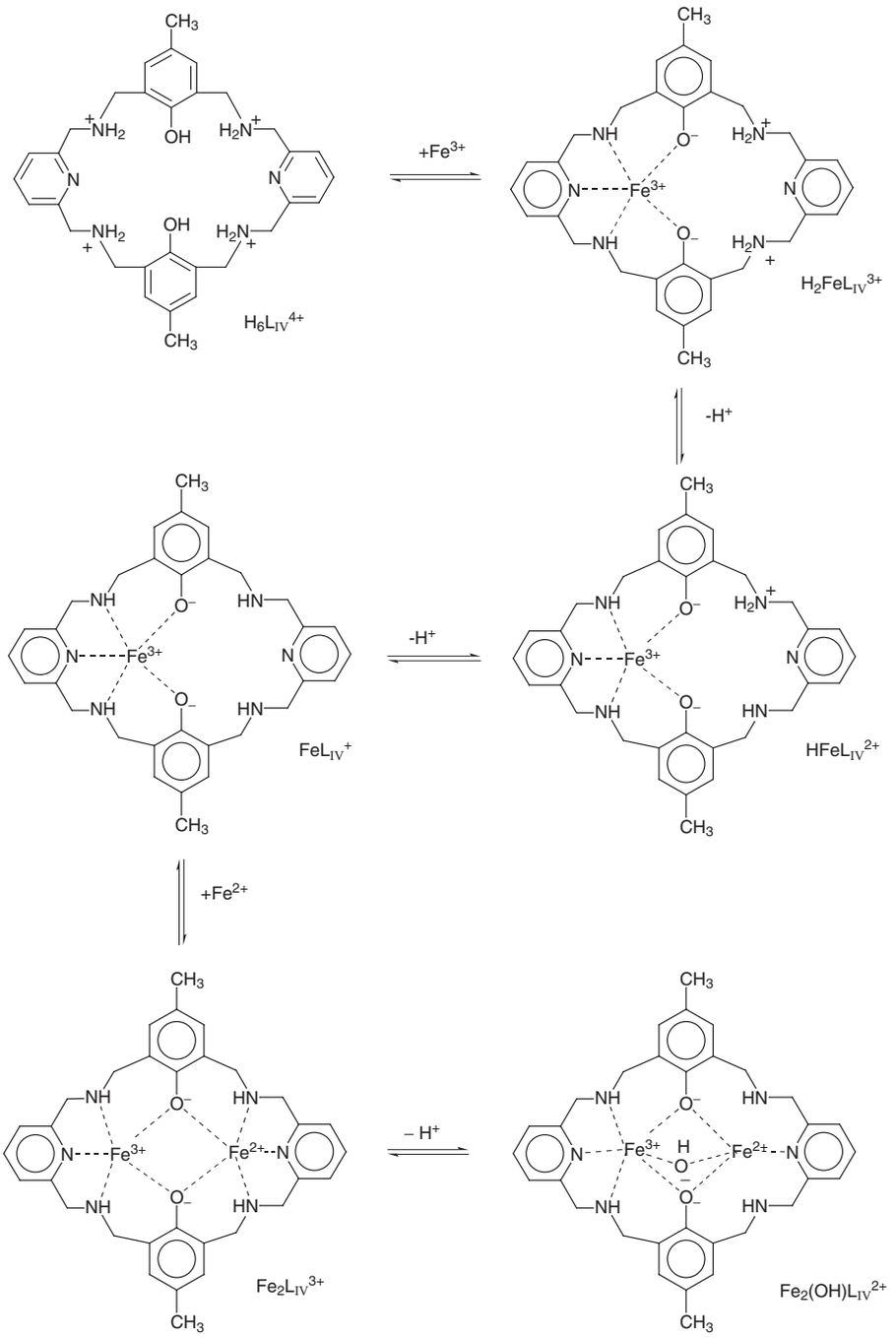

Scheme 2 Mixed-valence diiron(III, II) complexes formed with $H_6L_{IV}^{4+}$.

spectrometer, and by electrospray ionization with a Vestec 201 ESI quadrupole mass spectrometer at the Mass Spectrometry Applications Laboratory, Texas A&M University.

Electronic spectra were recorded at 25.0 °C with a Perkin-Elmer 553 Fast-Scan spectrophotometer equipped with 1.000 ± 0.001 cm matched quartz cells. The solutions were generally 10^{-4} M. Stability constants were calculated from spectral data with the help of short programs written in Basic utilizing mass balance and equilibrium constant equations by minimizing the least-squares absorbances fit to the observed absorbances at a prominent wavelength over a series of samples.

Preparation of ligand for potentiometric titration

The 2 + 2 condensation of 2,6-diformylpyridine with 2,6-bis(aminomethyl)-*p*-cresol, followed by hydrogenation with $NaBH_4$, was used to synthesize the hexaazadiphenol macrocyclic ligand.[9] The free ligand H_2L_{IV} (2.2 g, 4.0 mmol) was dissolved in 60 mL 5% HCl methanolic solution and then filtered. The filtrate was stored at 4 °C for 24 h and a white solid deposited. The product was collected by filtration, washed with cold methanol, and dried for 12 h at 65 °C under vacuum. 1.8 g product of $H_2L_{IV}\cdot4HCl\cdot1/3CH_3OH\cdot5/3H_2O$ was obtained (F.W. = 725, Yield = 62%). The purity of the sample and the HCl content were determined by potentiometric titration and elemental analysis. The CH_3OH content was checked by recording the ^1H NMR spectrum in D_2O. Anal. Calc. for $C_{32.33}Cl_4H_{46.67}N_6O_4$: C, 53.55; H, 6.49; N, 11.59; Cl, 19.55. Found: C, 53.50; H, 6.49; N, 11.57; Cl, 19.53. ^1H NMR (D_2O), δ: 2.32 (s, CH_3, 6H), 4.38 (s, CH_2, 8H), 4.57 (s, CH_2, 8H), 7.32 (s, aryl in cresol, 4H), 7.51 (d, aryl in pyridine, J = 8.0 Hz, 4H), and 7.94 (t, aryl in pyridine, J = 8.0 Hz, 2H). Mass spectrum (FAB^+): *m/z* 539 ($[H_2L_{IV}+H]^+$).

Isolation of crystalline ligand $H_2L_{IV}\cdot4HCl\cdot6CH_3OH$, 1

In order to obtain a crystalline sample, the above solid product (0.30 g, 0.41 mmol) was redissolved in 50 mL methanol and the

solution was filtered. The filtrate was heated to 60°C to reduce the volume by half and allowed to evaporate at room temperature for 3 days to afford colorless single crystals of the ligand as a tetrahydrochloride hexamethanol solvate, $H_2L_{IV}\cdot 4HCl\cdot 6CH_3OH$ **1**, which was suitable for X-ray diffraction study.

Potentiometric determinations

A Corning Model 350 pH meter fitted with a blue-glass electrode and a calomel reference electrode was calibrated with standard dilute strong acid at 0.10 M ionic strength to read hydrogen concentration directly so that the measured quantity was $-\log[H^+]$, designated as p[H]. Hydrogen ion activities (pH) were not employed in this research.

Potentiometric p[H] measurements and computation of the protonation constants and the stability constants of the iron complexes were carried out by procedures described in detail elsewhere.[15] The p[H] measurements were made at 25.00 ± 0.05 °C and ionic strength 0.10 M adjusted with KCl. Typical concentrations of experimental solutions were 2.20×10^{-3} M ligand and 0.100 M KOH as titrant. Typical initial solution volumes were 50.0 mL. The range of accurate p[H] measurement was considered to be 2–12. For the ligand the first and second protonation constants were determined spectrophotometrically. The third, fourth, fifth, and sixth protonation constants were determined by the direct titration. The stoichiometry of L_{IV}–Fe(II) and L_{IV}–Fe(III) systems were 1:1 and 1:2, with a slight (*ca.* 2%) excess of the ligand. The ternary system containing L_{IV}, Fe(II), and Fe(III) was studied at the molar ratio of 1:1:1. All systems were investigated under anaerobic conditions; oxygen and carbon dioxide were excluded from the reaction mixture by maintaining a slight positive pressure of purified argon gas in the reaction cell. Each titration was repeated at least 2 times and over 80 points were collected per titration.

Computations were all carried out with the program BEST.[15] The log K_w defined as $\log([H^+][OH^-])$, was found to be −13.78 at the ionic strength employed and was maintained fixed during refinements. The preliminary 1:1 stability constants were calculated from the equilibrium data of the 1:1 systems. The formation constants of the 1:2 complexes were then calculated from 1:2 titration data with the inclusion of the preliminary constants from the 1:1 systems. A more detailed refinement of the constants of the 1:1 system was then carried out while including the formation constants of the binuclear complexes obtained from the 1:2 systems. The procedure was repeated until the differences between the calculated and observed values of $-\log [H^+]$ were minimized for the potentiometric data of both the 1:1 and 1:2 complexes. Similar procedures were also followed for the calculations of the 1:1:1 ternary systems. Species distributions were calculated from the equilibrium constants with the help of program SPE[15] and plotted with SPEPLOT.[15]

Determination of high protonation constants

Because of the extremely high pK_a's of the phenolic groups and low solubility of the ligand containing hydrophobic aromatic rings, the values for two protonation constants had to be determined from the analysis of UV-visible spectral measurements made as a function of the amount of incremental alkali needed to raise the p[H] to about 13. A series of solutions containing appropriate concentrations of KOH and KCl ([KOH] + [KCl] = 0.100 M), and with each 1.10×10^{-4} M in ligand concentration, were measured between 260 and 360 nm, with matched 1.000 cm quartz cells and a thermostat set at 25.0 °C. In addition, several solutions were prepared with measured higher concentrations of KOH in order to help determine the ultimate molar absorbance of the totally deprotonated ligand. This was necessary because the protonation constants are too high to carry out the extrapolation to complete dissociation with measurements limited to an ionic strength of 0.100 M. The calculations involved the least-squares minimization of calculated *versus* observed absorbances through the variation of the first and second protonation constants as well as the second extinction coefficient corresponding to fully protonated phenolic groups. From the appropriate simultaneous equations for mass balance and total absorbance: the elimination of $[L^{IV}]$ gives:

$$T_{L_{IV}} = [L_{IV}](1 + K_1[H] + K_1K_2[H]^2) \quad (3)$$

$$A = [L_{IV}](\varepsilon_{L_{IV}} + \varepsilon_{HL_{IV}}K_1[H] + \varepsilon_{H_2L_{IV}}K_1K_2[H]^2) \quad (4)$$

$$A = T_{L_{IV}}(\varepsilon_{L_{IV}} + \varepsilon_{HL_{IV}}K_1[H] + \varepsilon_{H_2L_{IV}}K_1K_2[H]^2)/(1 + K_1[H] + K_1K_2[H]^2) \quad (5)$$

where $\varepsilon_{L_{IV}}$, $\varepsilon_{HL_{IV}}$, and $\varepsilon_{H_2L_{IV}}$ are the extinction coefficients of L_{IV}^{2-}, HL_{IV}^{-}, and H_2L_{IV}, respectively, and K_1 and K_2 are the two stepwise protonation constants leading to the HL_{IV}^{-} and H_2L_{IV} species from the fully deprotonated ligand L^{2-}. The wavelength chosen is near 300 nm, the characteristic wavelength of the phenolate absorbance maximum.

Table 5 Summary of crystallographic data for complex **1**

Formula	$C_{38}H_{66}N_6O_8Cl_4$
Formula weight	876.76
Space group	Triclinic, $P\bar{1}$
a/Å	9.2906(11)
b/Å	9.4416(13)
c/Å	14.332(2)
α/°	76.417(11)
β/°	73.912(10)
γ/°	71.765(10)
V/Å^3	1132.1(3)
Z	1
D_c/g cm^{-3}	1.286
μ/mm^{-1}	0.315
λ/Å	0.71073
T/K	193(2)
$R(F)$ [a]	0.0772
w$R(F^2)$ [b]	0.1498
GOF(F^2) [c]	1.017

[a] $R(F) = \Sigma||F_o| - |F_c||/\Sigma F_o$. [b] $wR(F^2) = \{[\Sigma w(F_o^2 - F_c^2)^2]/[\Sigma w(F_o^2)^2]\}^{\frac{1}{2}}$. [c] $\mathrm{GOF}(F^2) = \Sigma w(F_o^2 - F_c^2)^2/(N_D - N_P)$, N_D = number of data, N_P = number of parameters.

X-Ray structure analysis

Crystal data for complex **1** are given in Table 5. A colorless parallelepiped (0.42 × 0.31 × 0.14 mm) of **1** was mounted on a glass fiber with epoxy cement at room temperature. Preliminary examination and data collection were performed on a Rigaku AFC-5R X-ray diffractometer (Mo-Kα $\lambda = 0.71073$ Å radiation). Cell parameters were calculated from the least-squares fit of the angles for 25 reflections. Data were collected with $3.6 \leq 2\theta \leq 50°$ at 293 K. Three control reflections collected every 97 reflections showed no significant trends. Lorentz and polarization corrections were applied to 4201 reflections. A semi-empirical absorption correction was applied. A total of 3936 unique reflections was obtained. The structure was solved by direct methods.[16] Full-matrix least-squares anisotropic refinements[17] for all non-hydrogen atoms yielded $R = 0.0772$, w$R(F^2) = 0.1498$, and GOF = 1.017 at convergence. Hydrogen atoms were placed in idealized positions with isotropic thermal parameters fixed at 0.08 Å^2. Neutral atom scattering factors and anomalous scattering correction terms were taken from ref. 18. Positional parameters and the packing diagram of **1** are given in the Supplementary Material.

CCDC no. 186/1487.

Acknowledgements

This research was supported by the Robert A. Welch Foundation through Grant A-259. The crystallographic

computing system in the Crystal and Molecular Structure Laboratory of the Department of Chemistry, Texas A&M University, were purchased from funds provided by the National Science Foundation (Grant CHE-8513273). We thank Dr Abraham Clearfield, Texas A&M University, for use of the AFC5R X-ray diffractometer and thank Dr Lloyd W. Sumner for his assistance with the mass spectral analyses.

References

1 (*a*) J. B. Vincent, G. L. Olivier-Lilley and B. A. Averill, *Chem. Rev.*, 1990, **90**, 1447; (*b*) J. D. Lipscomb, *Annu. Rev., Microbiol.*, 1994, **48**, 371.

2 (*a*) R. H. Holm, P. Kennepohl and E. I. Solomon, *Chem. Rev.*, 1996, **96**, 2239; (*b*) A. L. Feig and S. J. Lippard, *Chem. Rev.*, 1994, **94**, 759; (*c*) K. D. Karlin, *Science*, 1993, **261**, 701.

3 (*a*) A. Stassinopoulos, S. Mukerjee and J. P. Caradonna, *Mechanistic Bioinorganic Chemistry*, Plenum Press, New York, 1995, p. 84; (*b*) V. McKee, *Adv. Inorg. Chem.*, 1993, **40**, 323.

4 W. H. Armstrong, A. Spool, G. C. Papaefthymiou, R. B. Frankel and S. J. Lippard, *J. Am. Chem. Soc.*, 1984, **106**, 3653; (*b*) K. Wieghardt, K. Pohl and W. Gebert, *Angew. Chem., Int. Ed. Engl.*, 1983, **22**, 727; (*c*) S. Menage, Y. Zhang, M. P. Hendrich and L. Que, Jr., *J. Am. Chem. Soc.*, 1992, **114**, 7786; (*d*) N. Kitajima, H. Fukui and H. Moro-oka, *J. Chem. Soc., Chem. Commun.*, 1988, 485.

5 (*a*) A. S. Borovik and L. Que, Jr., *J. Am. Chem. Soc.*, 1998, **110**, 2345; (*b*) V. D. Campbell, E. J. Parsons and W. T. Pennington, *Inorg. Chem.*, 1993, **32**, 1773; (*c*) M. Suzuki, A. Uehara, H. Oshio, K. Endo, M. Yanaga, S. Kida and K. Saito, *Bull. Chem. Soc. Jpn.*, 1987, **60**, 3547.

6 C. L. Spiro, S. L. Lambert, T. J. Smith, E. N. Duesler, R. R. Gagne and D. N. Hendrickson, *Inorg. Chem.*, 1981, **20**, 1229; (*b*) H. S. Mountford, D. B. MacQueen, A. Li, J. W. Otvos, M. Calvin, R. B. Frankel, L. O. Spreer, *Inorg. Chem.*, 1994, **33**, 1748; (*c*) R. J. Motekaitis, W. B. Utley and A. E. Martell, *Inorg. Chim. Acta*, 1993, **212**, 15.

7 (*a*) S. K. Mandal, L. K. Thompson, K. Nag, J. P. Charland and E. J. Gabe, *Inorg. Chem.*, 1987, **26**, 1391; (*b*) R. Das, K. K. Nanda, K. Venkatsubramanian, P. Paul and K. Nag, *J. Chem. Soc., Dalton Trans.*, 1992, 1253; (*b*) K. K. Nanda, S. K. Dutta, S. Baitalik, K. Venkatsubramanian and K. Nag, *J. Chem. Soc., Dalton Trans.*, 1995, 1239; (*d*) S. Dutta, R. Werner, S. Mohanta Florke, K. K. Nanda, W. Haase and K. Nag, *Inorg. Chem.*, 1996, **35**, 2292; (*e*) K. K. Nanda, L. K. Thompson, J. N. Bridson and K. Nag, *J. Chem. Soc., Chem. Commun.*, 1994, 1337.

8 R. M. Smith, A. E. Martell and R. J. Motekaitis, *Critical Stability Constants Database*, Version 4, NIST, Gaithersburg, MD, USA, 1993.

9 Z. Wang, J. Reibenspies and A. E. Martell, *Inorg. Chem.*, 1997, **36**, 629.

10 The complexity of the ligands discussed here requires that nomenclature now in use be revised (refer to N. F. Curtis, *Coord. Chem. Rev.*, 1968, **3**, 3 and J. C. Dabrowiak, P. H. Merrell and D. H. Busch, *Inorg. Chem.*, 1982, **11**, 1979; and compare reference 7 and reference 9). In order to represent these and more complicated ligands by convenient abbreviations we are recommending a new abbreviation system based in part on the starting materials of bis(primary amines) and dialdehydes used for preparation of macrocyclic ligands. In this system the internal ring size of the macrocyclic ligand is indicated by a number in brackets. In the absence of any unsaturated Schiff base bonds the heading "R" is adopted to indicate that all Schiff base bonds are reduced. Substituents, heteroatoms and azomethine linkages may be indicated with or without positions depending on the information that needs to be conveyed. For example the abbreviation for ligand 20,41-dimethyl-3,16,24,27,43,44,46,47-octaazaheptacyclo-[37.3.1.1.^{5,9}1.^{10,14}1.^{18,22}1.$^{26.30}$1.^{31,35}]-octatetraconta-5,7,9(43)12,12, 14(44),18,20,22(45),26,28,30(46)31,33,35(47)39,41,1(48)-octa-decaene-45,48-diol (see Fig. 1) then becomes [30]RBBPyBC (B = bis, BPy = bipyridine, and C = cresol). The abbreviation for ligand 15,31-dimethyl-3,11,19,27,33,35-hexaazapentacyclo-[27.3.1.1.^{5,9}1.^{13,17}1.^{21,25}]-hexatriconta-3,5,7,9(33),10,13,15,17(34),19, 21,23,25(35),26,29,31,1(36)-hexacaene-34,36-diol becomes [24]-1,6,13,18-tetraSb-BPyBC (Sb = Schiff base). These represent relatively complex abbreviations and often could be shortened further, for example, [24]BPyBC for [24]-1,6,13,18-tetraSb-BPyBC. Since the subject of this paper deals almost exclusively with metal complexes of 15,31-dimethyl-3,11,19,27,33,35-hexaazapentacyclo-[27.3.1.1.^{5,9}1.^{13,17}1.^{21,25}]-hexatriaconta-5,7,9(33),13,15,17(34),21,23, 25(35),29,31,1(36)-dodecaene-34,36-diol, the short abbreviation ([24]RBPYBC or the dianion, L_{IV}^{2-}) is used. Our system is designed to use the simplest abbreviation that contains the necessary structural information in the context of the discussion that is at hand. While these abbreviations are still more cumbersome than we might like, they are short enough to use in tabulated entries and one can derive from them much pertinent structural information.

11 G. C. Pimentel and A. L. McClellan, *The Hydrogen Bond*, Reinhold, New York, 1960, p. 290.

12 (*a*) F. L'Eplattenier, I. Murase and A. E. Martell, *J. Am. Chem. Soc.*, 1967, **89**, 837; (*b*) R. J. Motekaitis, A. E. Martell and M. J. Welch, *Inorg. Chem.*, 1990, **29**, 1463; (*c*) M. G. Basallote and A. E. Martell, *Inorg. Chem.*, 1988, **27**, 4219.

13 M. Suzuki, H. Oshio, A. Uehara, K. Endo, M. Yanaga, S. Kida and K. Saito, *Bull. Chem. Soc. Jpn.*, 1988, **61**, 3907.

14 Z. Wang, A. E. Martell and R. J. Motekaitis, *Chem. Commun.*, 1998, 1523.

15 A. E. Martell and R. J. Motekaitis, *The Determination and Use of Stability Constants*, VCH Publishers, New York, 2nd edn., 1992.

16 G. M. Sheldrick, SHELXS 86, Program for Crystal Structure Solutions, University of Göttingen, Germany, 1986.

17 G. M. Sheldrick, SHELXS 93, Program for Crystal Structure Solutions, University of Göttingen, Germany, 1993.

18 T. Hahn and D. Reidel, *International Tables for X-ray Crystallography*, Vol. C, distributed by Kluwer Academic Publishers, Dordrecht, 1992.

Paper 8/08051H